

Progress Report

May 2001

Simon J. Hook
Fred J. Prata
Geoffrey S. Schladow

(<http://shookweb.jpl.nasa.gov/validation>)

Table of Contents

Introduction.....	4
Instrument Development.....	4
Site Status.....	5
Lake Tahoe, CA, USA.....	5
Thangoo, WA, Australia.....	5
Amburla NT, Australia.....	5
Uardry, NSW, Australia.....	6
Validation Strategy.....	7
Validation Procedure.....	8
Radiance at Sensor Product.....	8
Surface Temperature Product.....	12
Surface Emissivity Product.....	13
Validation Results.....	13
Radiance At Sensor Product (MOD021KM, AST01B).....	14
Surface Temperature Product (MOD11_L2, AST08).....	16
Surface Emissivity Product (MOD11_L2, AST08).....	18
Validation Summary Tables.....	19
Future Plans.....	22
Schedule.....	23
Publications and Media.....	23
Collaborations.....	24
Archiving.....	25
WebPages.....	25
References.....	25

List of Figures

Figure 1. Plot showing the variation in the bulk-, skin-, air-temperatures and wind speed for June 7, 2001 at L. Tahoe.	11
Figure 2. Predicted satellite brightness temperatures (field derived) minus measured (satellite) brightness temperatures for a typical MODIS validation on May 29, 2000 for the 4 rafts at Lake Tahoe and MODIS channels 28-29 and 30-33.....	14
Figure 3 Average temperature difference between the Predicted (field derived) and measured (satellite) MODIS at sensor brightness temperatures over time for CY2000.....	15
Figure 4 Average temperature difference between the Predicted (field derived) and measured (satellite) ASTER at sensor brightness temperatures over time for CY2000.....	16
Figure 5. Temperature Difference between Predicted (ASTER) and Measured (Field Radiometer) Values over Time CY2000 v1.0.2.	17
Figure 6. Daytime MODIS scene acquired over Lake Tahoe on 3/12/2000. Image on left is a grayscale brightness temperature image from the band 31 and image on right is the MODIS surface temperature product.....	18
Figure 7. Emissivity Difference between ASTER Predicted and Measured Values over Time CY2000 v1.0.2.....	19

List of Tables

Table 1. MODIS and ASTER channels currently being validated. Preflight calibration accuracy requirements for MODIS and ASTER are obtained from Barnes et al., 1998 and Fujisada et al., 1998. The accuracy requirement outside the 270-340 K range is not listed since all the validation data fall within the 270-240 K range.....	8
Table 2. MODIS and ASTER overpasses validated at Lake Tahoe. Each scene includes 4 independent validation values giving a total number of 40 validation points for MODIS.....	13
Table 3. Preflight and Validated Accuracy of the ASTER and MODIS radiance at sensor products for nadir viewed scenes. Preflight calibration accuracy requirements for MODIS and ASTER are obtained from Barnes et al., 1998 and Fujisada et al., 1998.	20
Table 4 Preflight and Validated Accuracy of the ASTER surface temperature product (AST08) over water. Preflight accuracy requirement obtained from Gillespie et al. 1998.....	21
Table 5 Preflight and Validated Accuracy of the ASTER surface emissivity product (AST08) over water. Preflight accuracy requirement obtained from Gillespie et al. 1998.....	22

Introduction

In 1997 a proposal was submitted to the Satellite Remote Sensing Measurement Accuracy, Variability, and Validation Studies NASA Research Announcement entitled:

“Validation of Thermal Infrared Data and Products from MODIS and ASTER over Land”

The objective of the proposal was to validate the thermal infrared data and products acquired over land from the Advanced Spaceborne Thermal Emission Reflectance Radiometer (ASTER) and the Moderate Resolution Imaging Spectroradiometer (MODIS) using a set of automated validation sites. The main advantage of this approach is the validation data are acquired automatically allowing validation whenever satellite data are acquired and monitoring of accuracy and precision of the satellite data and products over time. The proposal was accepted and 4 automated validation sites were identified. The sites were chosen to encompass a range of cover types and atmospheric conditions. The sites were L. Tahoe, CA, USA; Thangoo, WA, Australia; Amburla, NT, Australia and Uardry, NSW, Australia. The subsequent report is divided into the following main sections: Instrument Development, Site Status, Validation Strategy, Validation Procedure, Validation Results, Validation Summary Tables, Future Plans and Schedule, Publications and Media, Collaborations, Archiving. The Instrument Development section summarizes work on the radiometers used to measure the surface skin temperature. The Site Status section provides a brief status of each site noting any changes for the reporting year. The Validation Strategy describes the approach used to select scenes and products for validation. The Validation Procedure section summarizes the procedure used to validate each of the products. The Validation Results section provides some examples of validation results for a particular overpass as well as for all the scenes validated to date. The Validation Summary section provides an assessment of the in-flight accuracy of the various products compared to the expected (preflight) accuracy. The Future Plans and Schedule section covers the equipment plans for the sites and future validation work. The Collaboration section describes how the sites have been incorporated into the work of other Instrument teams. The Archiving section discusses how the field data are being archived.

Instrument Development

The primary instrument development associated with this project is the ongoing improvement of the CSIRO and JPL developed radiometers for measuring the surface skin temperature. Similar radiometer developments are underway by the sea surface temperature community, such as the SISTeR radiometer developed by Tim Nightingale at the Rutherford Appleton Laboratory (UK). The sea surface radiometers are designed for use from research vessels. They are large, heavy, have significant power requirements and designed to withstand the rigors of deployment in a saltwater environment. By contrast, the CSIRO and JPL radiometers are light, small, have low power requirements and are currently only suitable for deployment in freshwater environments such as Lake Tahoe or on land.

Early in 2001 work was completed on the new JPL Mk III near-nulling radiometer. These radiometers have an accuracy of ± 0.05 K compared to the Mk II radiometers, which have an accuracy of ± 0.2 K. The improved accuracy is achieved by having the radiometer periodically view a very accurate internal blackbody maintained at the same temperature as the scene. This blackbody measurement is then used to correct for any drift in the radiometer calibration. Mk III radiometers were deployed at Lake Tahoe in the spring of 2001. The performance of the JPL Mk III radiometers was also compared to other high accuracy radiometers developed by the sea surface temperature community at an Intercomparison Workshop at the Rosenstiel School of Marine and Atmospheric Sciences between May 28 and June 1, 2001. The workshop was organized by Peter Minnett at the University of Miami and included laboratory comparisons against the NIST blackbody and Thermal Infrared Transfer Radiometer as well as an overnight deployment from the University of Miami Research Vessel (R/V Walton Smith). Results from this intercomparison are available from <http://www.rsmas.miami.edu/ir2001>.

Site Status

Lake Tahoe, CA, USA

The Lake Tahoe validation site has been fully operational since June of 1999 when all four of the validation platforms were deployed. Since becoming operational, considerable effort has gone into maintaining the platforms due to several severe storms. The same storms resulted in the US Coast Guard pier, where the land instrumentation is deployed, sustaining damage and requiring rebuilding. It was necessary to remove the land instrumentation in order to rebuild the pier. The new pier was recently completed and the land instrumentation will be re-deployed in the fall of this year. The pier instrumentation provides valuable supplementary information but is not essential for the validation work.

In the spring of 2001 the new JPL Mk III near-nulling radiometers were deployed at the site (see section on Instrument Development above for further details).

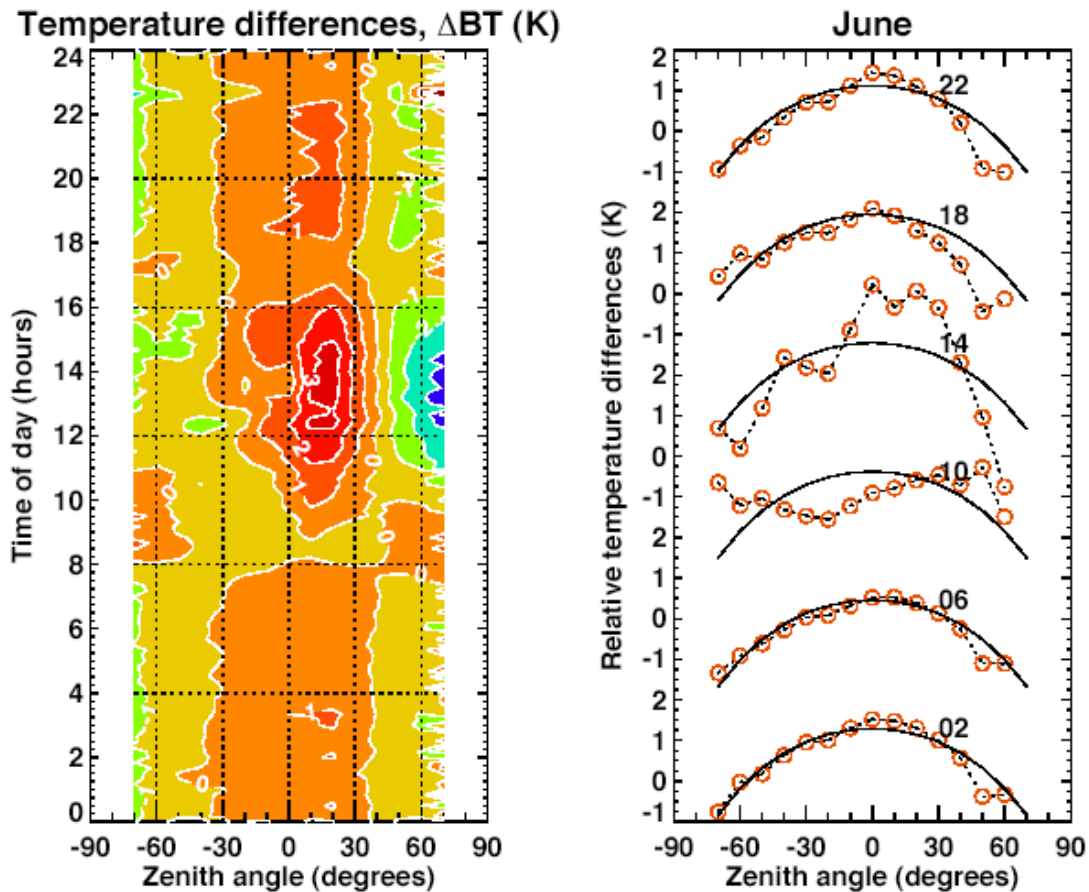
Thangoo, WA, Australia

The site was made fully operational in May 2001 following the end of the wet season and refurbishment of damaged equipment (see previous report). Three radiometers are operating at the site together with radiation instruments, meteorological instruments and routine collection of daily radiosonde data from the Broome aerodrome (about 40 km distant from the site). A complete site survey has been conducted, including a GPS survey and assessment of vegetation state and health.

Amburla NT, Australia

The site has been running with little interruption throughout the study period, starting in 1995. A single scanning radiometer was added to the site in May 2000. This has been operating exceptionally well and has provided new data on the angular variation of

emissivity at this sparsely vegetated site. The radiometer scans from -70 to $+70$ degrees through nadir, with one view of the sky to provide a correction for reflected sky radiation. After averaging these data over many days to remove solar heating and wind-induced thermal effects, a clear angular variation can be discerned in the nighttime data. The Figure below shows some results, where it can be seen that at 0200, 0600, 1800 and 2200 hours local time there is a strong variation of the brightness temperature with angle. We have modelled this variation and found that it can be reproduced by theoretical modelling of the surface emissivity. During the day the angular variation is masked by significant differential solar heating of the surface and by shading effects.



These data will prove useful in assessing the surface temperature and emissivity products from MODIS and ASTER at off-nadir view angles.

Uardry, NSW, Australia

Four radiometers are now operating at the Uardry site and these have been a great success. Three radiometers measure at off-nadir angles (up to 55°), while one radiometer views the surface at nadir.

Validation Strategy

The strategy adopted to validate the MODIS and ASTER data and products was to first validate the radiance at sensor data and then validate the derived surface products (radiance, temperature, emissivity). The Lake Tahoe site has certain attributes that make it suitable for validation of both the radiance at sensor and the surface derived products, whereas the Australian sites are more suitable for validating the derived surface products. Therefore, the initial validation efforts have been focused on data acquired over Lake Tahoe. (The attributes of the automated validation sites are documented in the earlier status reports.)

Given the focus on Lake Tahoe, the next step was to identify those dates for which both MODIS and ASTER data were available at Lake Tahoe. The advantage of utilizing simultaneous acquisitions is they provide an opportunity to validate two spaceborne instruments using the same field data, thereby removing any potential variation due to differences in the time of measurement between the instruments. Since Lake Tahoe is centered on a Terra orbit track and ASTER is an on-demand instrument with a revisit time of 16 days whereas MODIS has a revisit time of every 2 days this approach reduced the number of potential MODIS scenes available for validation and focused the validation efforts on scenes viewed close to nadir. Every effort was taken to get as many ASTER acquisitions as possible over Lake Tahoe since it is an on-demand instrument and this resulted in a reasonable number of cloud-free scenes. Future work will focus on expanding the number of MODIS scenes to include dates when only MODIS data were available at both nadir and off-nadir view angles. In order to utilize data from different view angles it is necessary to include an emissivity model to account for changes in surface emissivity with view angle. Such models are being incorporated into the validation procedures. They typically require information on wind speed as well as view angle and this information is now available with the addition of a meteorological station to one of the western rafts. A meteorological station will be added to one of the eastern rafts in the fall of 2001.

Next the Lake Tahoe scenes were visually inspected and any cloud-contaminated scenes were excluded. Once the cloud free scenes were selected the data from each instrument was reprocessed to a common calibration version to ensure differences in the validation results were not due to changes in the calibration coefficients. Both MODIS and ASTER have updated the coefficients used to calibrate the data based on the instrument calibration teams understanding of the instrument behavior over time. In this report all MODIS data were reprocessed to version 2.5.4 and all ASTER data were reprocessed to version 1.02. It should be noted at the present time it takes 2-4 months to get a small number of MODIS scenes (<10) reprocessed.

After reprocessing, the data from the clear "window" channels were extracted for validation. These channels are listed in Table 1. This table does not include MODIS channels 20-23 in the mid wave infrared (MWIR) which will be validated this year.

Instrument	Bands	Centroid Wavelength (um)	Spatial Resolution	Preflight Calibration Accuracy Requirement	NEAT Requirement
MODIS	29	8.53	1 km	<1%	0.05
MODIS	31	11.02	1 km	<1%	0.05
MODIS	32	12.03	1 km	<1%	0.05
ASTER	10	8.29	90 m	≤1 K (270-340 K)	
ASTER	11	8.63	90 m	≤1 K (270-340 K)	≤ 0.3
ASTER	12	9.08	90 m	≤1 K (270-340 K)	≤ 0.3
ASTER	13	10.66	90 m	≤1 K (270-340 K)	≤ 0.3
ASTER	14	11.29	90 m	≤1 K (270-340 K)	≤ 0.3

Table 1. MODIS and ASTER channels currently being validated. Preflight calibration accuracy requirements for MODIS and ASTER are obtained from Barnes et al., 1998 and Fujisada et al., 1998. The accuracy requirement outside the 270-340 K range is not listed since all the validation data fall within the 270-240 K range.

Validation Procedure

Radiance at Sensor Product

The procedure for validating the radiance at sensor product is summarized as the follows:

- 1) Obtain the interpolated NCEP atmospheric profile for the time of the overpass.
- 2) Correct the surface radiometric measurements to surface skin temperature.
- 3) Calculate the average bulk temperature for each raft.
- 4) Calculate the skin effect (difference between the average bulk and skin temperature).
- 5) Determine the skin temperature for rafts with bulk temperature values only.
- 6) Propagate the surface skin temperature to at-sensor radiance using the radiative transfer model (MODTRAN 3.5) driven by the atmospheric profile.
- 7) Convolve the modeled at-sensor radiance with the system response functions for the satellite radiometer.
- 8) Extract the satellite radiometer at-sensor radiance values over each of the rafts. For the MODIS data a 3x3 km area (3x3 pixels) was extracted. For ASTER a 270x270 m area (3x3 pixels) was extracted. The area extracted was centered on the location of each raft, which was determined by differential GPS.

- 9) Calculate the average difference between the predicted and satellite measured values.
- 10) Assess the accuracy of product over time.

Step (1) – Obtain the interpolated NCEP atmospheric profile for the time of the overpass

The atmospheric profile was obtained from the National Center for Environmental Prediction (NCEP). The NCEP produces global model values on a 1-degree by 1-degree grid at 6 hr intervals. Lake Tahoe is centered on 39 N, 120 W and the grid value for this point was utilized. The NCEP data were interpolated to the overpass time.

Step (2) – Correct the surface radiometric measurements to surface skin temperature

The JPL Mk II radiometers have 2 internal blackbodies and provided the internal blackbody temperatures bracket the scene, are accurate to ± 0.2 K. NIST traceability is provided by laboratory calibration of the radiometer against the JPL cone blackbody that was traced to NIST using their transfer radiometer (Kanneburg, 1998). The radiometers measure the radiative temperature of the skin of the lake over the 8-12 μm wavelength region and in order to obtain the skin (kinetic) temperature it is necessary to correct the data for any atmospheric and emissivity effects. The skin temperature is derived by correcting for surface emissivity and subtracting the sky radiance reflected by the surface into the path of the radiometer:

$$L_{obs} = \int_{\lambda} R(\lambda) \left[L_{path}(\lambda) + \tau(\lambda)\varepsilon(\lambda)L_{BB}(T, \lambda) + \tau(\lambda)(1 - \varepsilon(\lambda)) \frac{I_{sky}(\lambda)}{\pi} \right] d\lambda \quad \text{Equation 1}$$

Where:

L_{obs} = observed radiance at sensor

L_{BB} = blackbody radiance (Planck function)

L_{path} = emitted radiance from surface – sensor path

I_{sky} = total downwelling irradiance upon the surface

λ = wavelength

T = temperature

τ = surface – sensor path transmit tan ce

ε = surface emissivity

R = Normalized system spectral response function

The path transmittance, path radiance, and downwelling irradiance terms are obtained from a radiative transfer model (MODTRAN 3.5) driven by a supplied atmospheric profile obtained in Step (1). The emissivity of the water was obtained from the ASTER spectral library. With all terms of Equation 1 determined, the equation is solved for temperature by iteration. It should be noted the path transmittance terms and path radiance terms are for the 1m of air between the water surface and the radiometer. For a high altitude site with a dry atmosphere these terms are close to 1 and 0 respectively.

Step (3) Calculate the average bulk temperature for each raft

The bulk temperature is measured approximately 2 cm beneath the surface by several different types of temperature sensors. Initially, the temperature trace of each logger over time was examined to make sure the logger was reading correctly. This was necessary because the cables from the loggers occasionally developed leaks causing the temperature values to drift. The data from any suspect loggers were discarded and the two temperature values closest to the overpass time, for a given logger, were linearly interpolated to the acquisition time of the nadir pixel. The mean and standard deviation of the interpolated values for each raft was then calculated. Since the measurements are normally made every 2 minutes with a maximum of every 5 minutes the interpolation time is typically less than 2 minutes.

Step (4) Calculate the skin effect

The skin effect was calculated as the bulk temperature minus the skin temperature. The skin effect was typically less during the day than at night. The smaller skin effect observed in the daytime is attributed primarily to strong solar heating coupled with low wind speeds. However, other factors are important such as the difference between the air and water temperature. Figure 1 shows a plot of some recent field data acquired over Lake Tahoe at the TR3 station on June 7th 2001. These data were derived using the Mk III near-nulling radiometer and include simultaneous meteorological data. These data are from a calm day; notice that as the solar elevation increases (1600 GMT, 0800 PST), the bulk and skin temperature both increase, with the skin temperature increasing more rapidly and surpassing the bulk temperature until the early afternoon. In the early afternoon the wind increases, resulting in a reduction in the skin and bulk temperatures (shown by a double arrow on Figure 1). The morning increase in the bulk temperatures is also associated with an increase in the standard deviation of the bulk temperature measurements (not shown). The standard deviation of the bulk temperatures also decreases in the early afternoon as the wind increases due to greater mixing. In the late afternoon the wind speed decreases and a skin/bulk differential is established which remains fairly constant throughout the night. As the wind speed increases in the early afternoon, so does the air temperature as warm air from the adjacent land is blown over the lake. Days characterized by low wind speeds and strong solar heating occur predominantly in the spring and fall. These data illustrate the importance of measuring the skin (what the satellite measures) rather than bulk temperature which could be different by as much as ± 0.5 K.

Lake Tahoe Diurnal Cycle - 6/7/2001

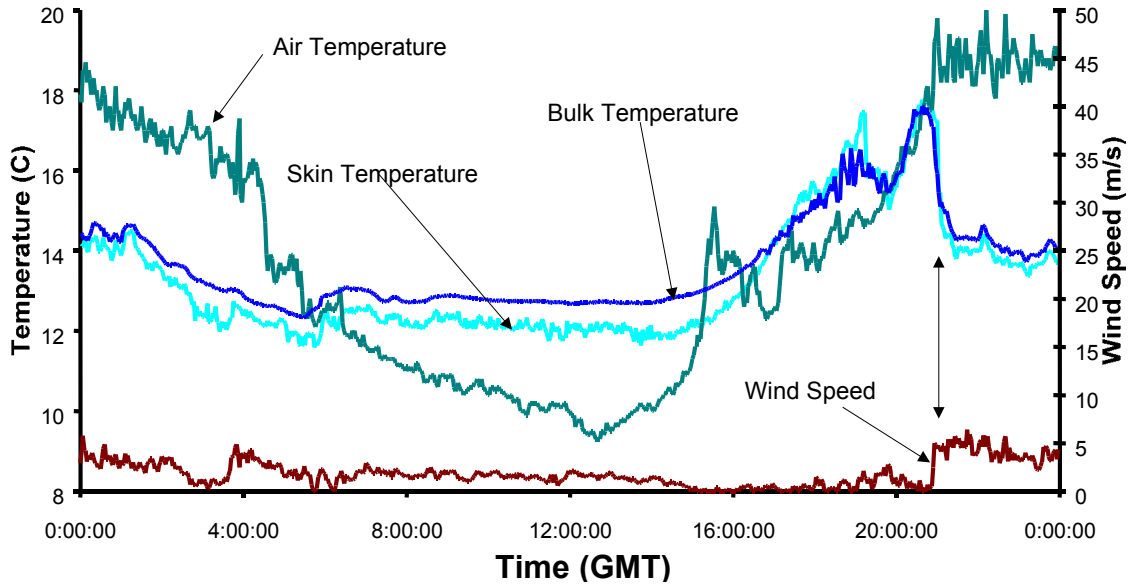


Figure 1. Plot showing the variation in the bulk-, skin-, air-temperatures and wind speed for June 7, 2001 at L. Tahoe.

Step (5) Determine the skin temperature for rafts with bulk temperature values only

In some cases, the radiometric temperature was not available at a given overpass or for a particular raft on a given overpass. If no radiometric temperatures were available from any of the rafts, the radiometric temperature was estimated by adding the average difference for all the overpasses to the bulk temperature at each raft. If radiometric temperatures were available at some of the rafts then the average difference of the available radiometric temperatures was calculated and added to the bulk temperatures of the rafts that had bulk measurements but no radiometric measurements to estimate the radiometric temperature at that raft.

Step (6) Propagate the surface skin temperature to at-sensor radiance

The at-sensor radiance was calculated using a radiative transfer code (MODTRAN 3.5) driven by the interpolated NCEP profile obtained in Step (1) and the derived surface skin temperature and emissivity of water.

Step (7) Convolve the modeled at-sensor radiance with the system response functions for the satellite radiometer

The high-resolution at-sensor radiance spectrum obtained in Step (6) was convolved to the sensor system response.

Step (8) Extract the satellite radiometer at-sensor radiance values over each of the rafts

For the MODIS data a 3x3 km area (3x3 pixels) was extracted. For ASTER a 270x270 m area (3x3 pixels) was extracted. The area extracted was centered on the location of each raft, which was determined by differential GPS

Step (9) Calculate the average difference between the predicted and satellite measured values

For each overpass day there would typically be 4 validation points (1 per raft). For each of these points the difference between the predicted (derived from ground measurement) and the satellite-measured values is calculated. These 4 values are then averaged to obtain an average difference between the predicted and measured values for a given overpass day.

Step (10) Assess the accuracy of product over time

See validation results.

Surface Temperature Product

The procedure for validating the surface temperature product is summarized as:

- 1) Obtain the interpolated NCEP atmospheric profile for the time of the overpass.
- 2) Correct the surface radiometric measurements to surface skin temperature.
- 3) Calculate the average bulk temperature for each raft.
- 4) Calculate the skin effect (difference between the average bulk and skin temperature).
- 5) Determine the skin temperature for rafts with bulk temperature values only
- 6) Extract the satellite derived surface temperature values over each of the rafts. For the MODIS data a 3x3 km area (3x3 pixels) was extracted. For ASTER a 270x270 m area (3x3 pixels) was extracted. The area extracted was centered on the location of each raft, which was determined by differential GPS.
- 7) Calculate the average difference between the predicted (derived from satellite) and ground measured values. Note the predicted values are now those derived from the satellite.
- 8) Assess the accuracy of product over time.

A detailed description of these steps is provided in the validation procedure for the at-sensor radiance product, where appropriate.

Surface Emissivity Product

The procedure for validating the surface emissivity product is summarized as:

- 1) Extract the satellite derived surface emissivity values over each of the rafts. For the MODIS data a 3x3 km area (3x3 pixels) was extracted. For ASTER a 270x270 m area (3x3 pixels) was extracted. The area extracted was centered on the location of each raft, which was determined by differential GPS.
- 2) Convolve a laboratory spectrum of emissivity to the system response function of the instrument. For water the emissivity spectrum is well known when nadir-viewed.
- 3) Calculate the average difference between the predicted (derived from satellite) and ground measured values. Note the predicted values are now those derived from the satellite.
- 4) Assess the accuracy of product over time.

Validation Results

MODIS and ASTER data acquired over Lake Tahoe during CY2000 have been used to validate the radiance at sensor, surface temperature and surface emissivity products of ASTER and MODIS. This section is separated into three parts based on these three products. The dates of MODIS and ASTER overpasses validated at Lake Tahoe are given in Table 2.

Date	D/N	Instruments
3/12/2000	D	Both
4/29/2000	D	MODIS only
6/24/2000	N	Both
7/2/2000	D	MODIS only
7/18/2000	D	MODIS only
8/4/2000	N	Both
8/19/2000	D	Both
9/20/2000	D	MODIS only
9/28/2000	N	Both
11/7/2000	D	Both

Table 2. MODIS and ASTER overpasses validated at Lake Tahoe. Each scene includes 4 independent validation values giving a total number of 40 validation points for MODIS.

Radiance At Sensor Product (MOD021KM, AST01B)

The results from a typical validation for MODIS are shown in Figure 2 for the MODIS thermal infrared channels (28-29 and 31-33). The difference between the predicted (field derived) and satellite measured brightness temperatures are shown for each of the rafts together with the average difference. Also shown are error bars in both the x and y direction. The x (horizontal) error bars are the average of the standard deviations of 3x3 MODIS pixels used to calculate the difference between the predicted and measured values. They provide an indication of the homogeneity of the 3x3 pixel area used. The y (vertical) error bars are the average of the difference between the predicted and measured values at each raft. They provide an indication of the amount of scatter in the 4 validation points in each scene. They also represent the typical error associated with a validation (including both the error from the radiometer and the forward calculation). They are typically around ± 0.3 K for the window channels, 29, 31, 32 (about 0.2 K error from the radiometer and 0.1 K error from the forward calculation).

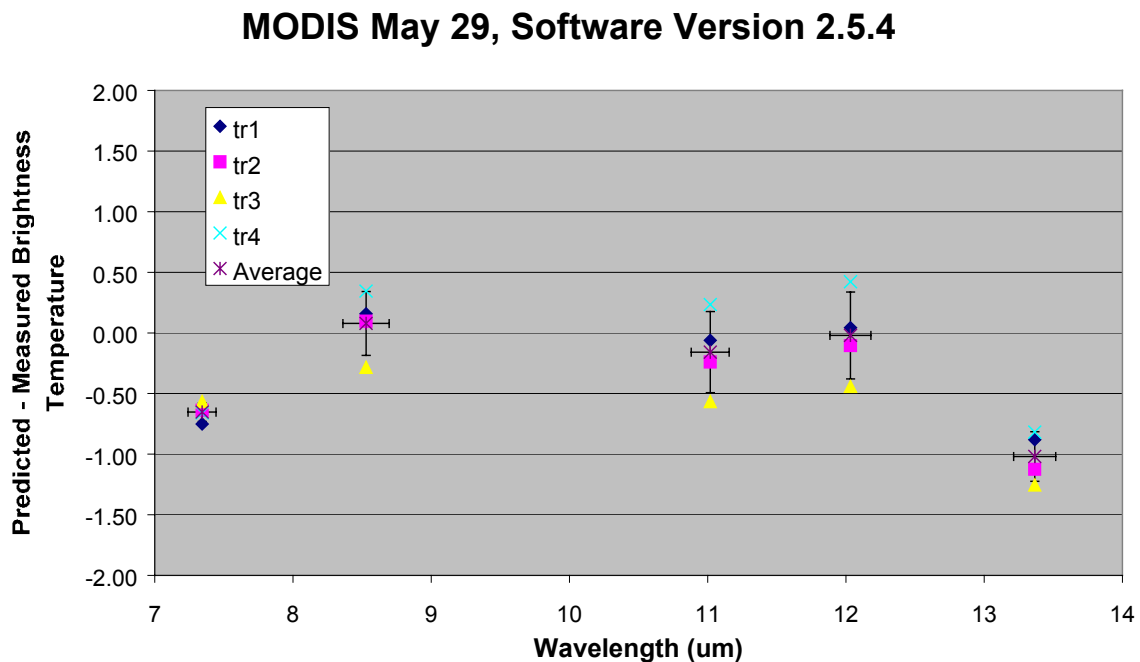


Figure 2. Predicted satellite brightness temperatures (field derived) minus measured (satellite) brightness temperatures for a typical MODIS validation on May 29, 2000 for the 4 rafts at Lake Tahoe and MODIS channels 28-29 and 30-33.

Although Figure 2 shows the results from channels 28 and 33 these channels are not normally validated since atmospheric effects dominate them. Examination of Figure 2

indicates the window channels (29, 31, 32) are within ± 0.3 of the predicted values (derived from the field data) for this particular overpass. Figure 3 shows the average temperature difference for the 3 MODIS window channels for the validated scenes listed in Table 2 and Figure 4 shows the equivalent plot for the 5 ASTER window channels.

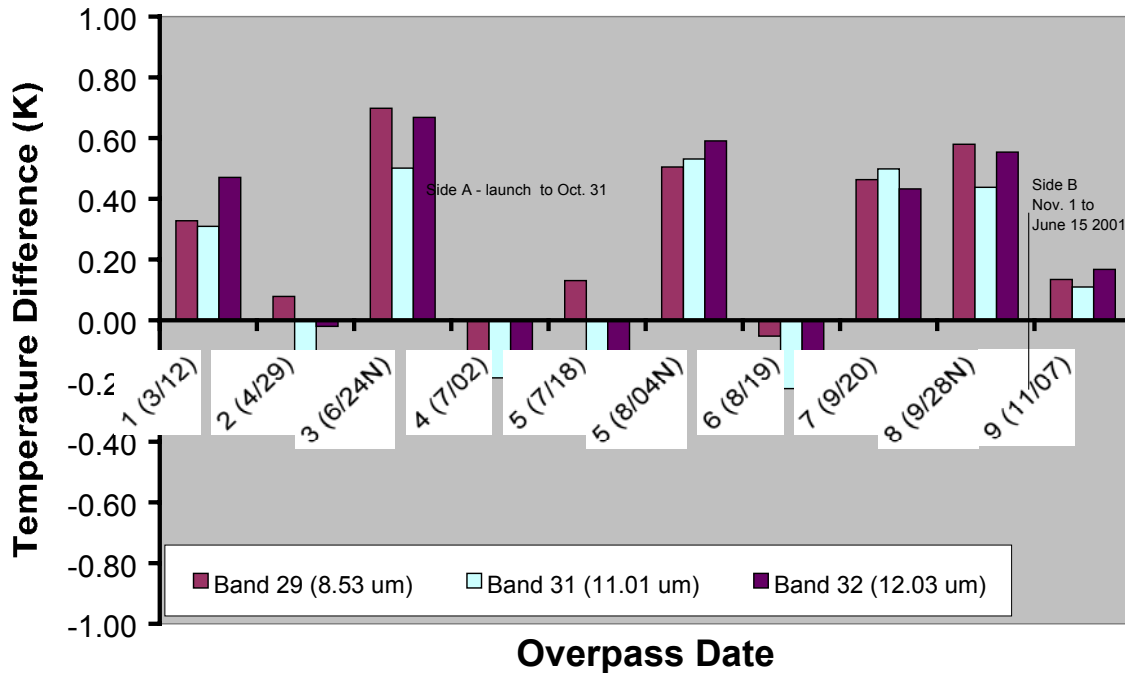


Figure 3 Average temperature difference between the Predicted (field derived) and measured (satellite) MODIS at sensor brightness temperatures over time for CY2000.

These plots provide an assessment of the accuracy of the at-sensor brightness temperature and the field data can be used to generate equivalent plots for the at-sensor radiance. From these we can determine the accuracy of each instrument over time. As more validations are completed it is hoped we will also be able to monitor small changes in the calibration over short time periods, such as the period when the MODIS focal plane warmed (between early June and early August) and its impact on the accuracy of the radiance at sensor product. These data have been used to produce summary tables of the accuracy of the radiance at sensor product for the MODIS and ASTER window channels and are presented in the subsequent section on Validation Summary Tables.

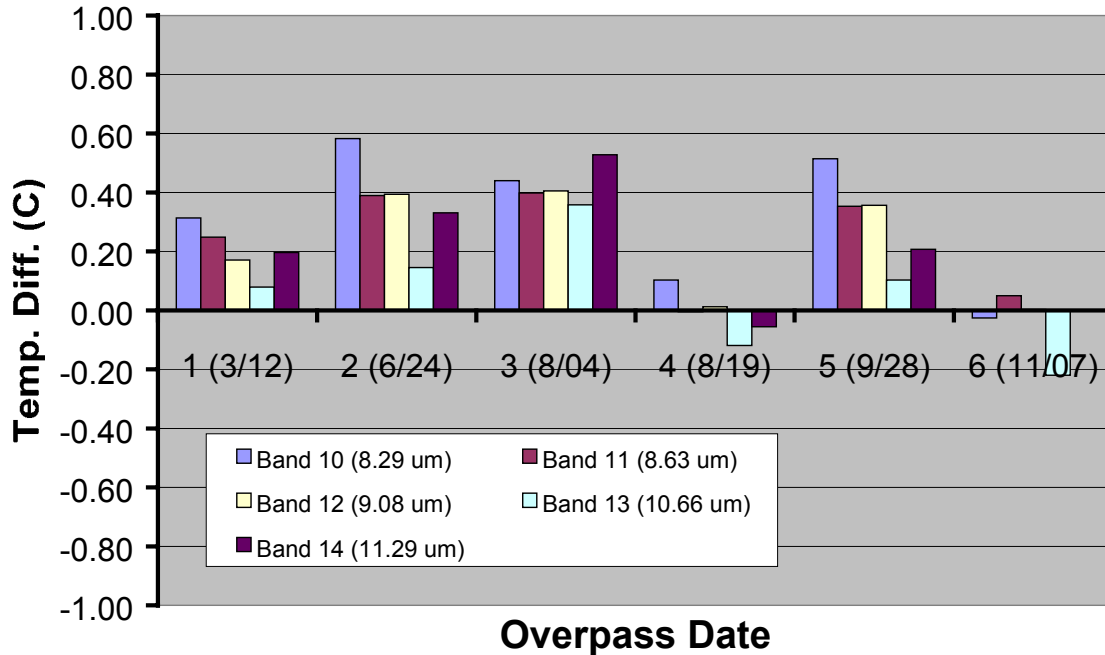


Figure 4 Average temperature difference between the Predicted (field derived) and measured (satellite) ASTER at sensor brightness temperatures over time for CY2000.

Surface Temperature Product (MOD11_L2, AST08)

The procedure for validating the surface temperature product was outlined in the previous section. Since the accuracy of the surface temperature product will vary with cover type and atmospheric conditions it is important to validate this product over a range of cover types and conditions. Thus far this product has been validated over one cover type: water. Other cover types include grassland (Uardry site) and bare soil (Amburla site). Other atmospheric conditions include the Thangoo site (high water vapor). Figure 5 illustrates the results of validating the ASTER surface temperature over Lake Tahoe. Examination of this figure indicates that for this cover type there is a bias (~ 0.9 K) but the product is very consistent over time.

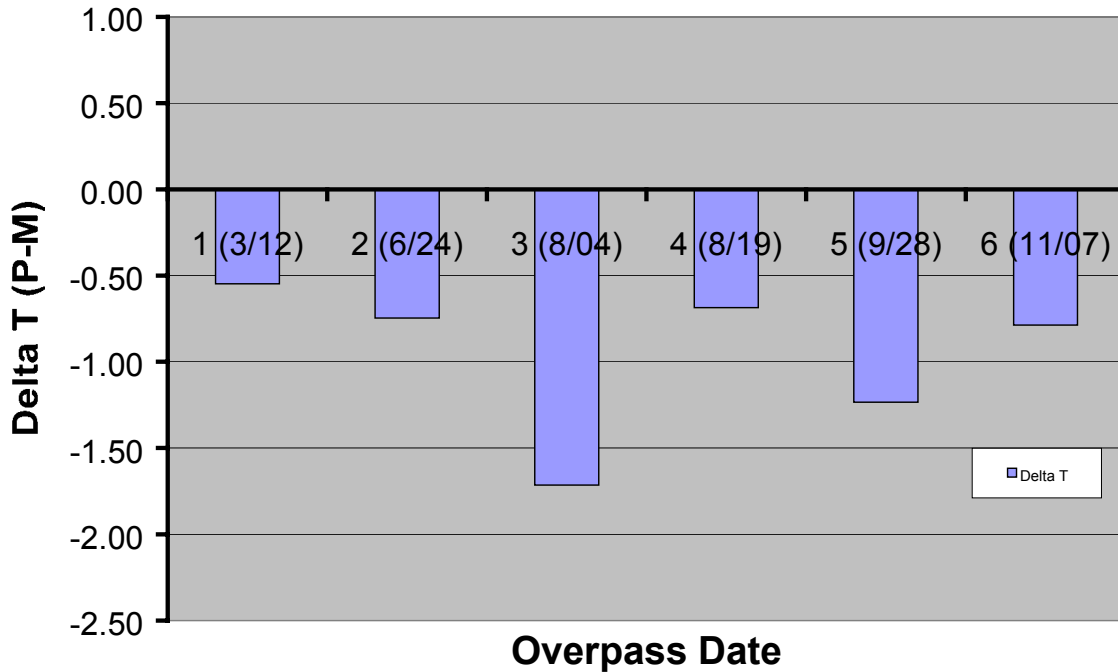


Figure 5. Temperature Difference between Predicted (ASTER) and Measured (Field Radiometer) Values over Time CY2000 v1.0.2.

A similar analysis was attempted on the MODIS surface temperature product but problems were encountered. The MODIS surface temperature algorithm only processes pixels that are classified as cloud-free at a confidence level of 99% by the cloud mask algorithm. In order to obtain this number the cloud mask algorithm performs a set of spectral tests on the data. One of these tests is for thin cirrus and over water the 11-12 μm thin cirrus test has slightly lowered confidences resulting in water pixels being classified as clear at the 95% confidence level. This means that on days when there are no visible clouds present in the scene, water is classified as clear at the 95% confidence level, and surface temperature retrievals are not performed for those pixels. This is illustrated in the next figure, which shows the surface temperature product in part of the southwest, including L. Tahoe on a day when Pyramid Lake was perfectly clear and Lake Tahoe had some contrails and clouds in the southern part of the lake. Notice how there were no retrievals over Pyramid Lake or Lake Tahoe since both bodies of water were classified as 95% cloud-free. Also notice how large parts of the desert region in the northeast of the image were also not processed because again there were classified as clear at the 95% confidence level or less since there are problems with the cloud mask over bright targets.

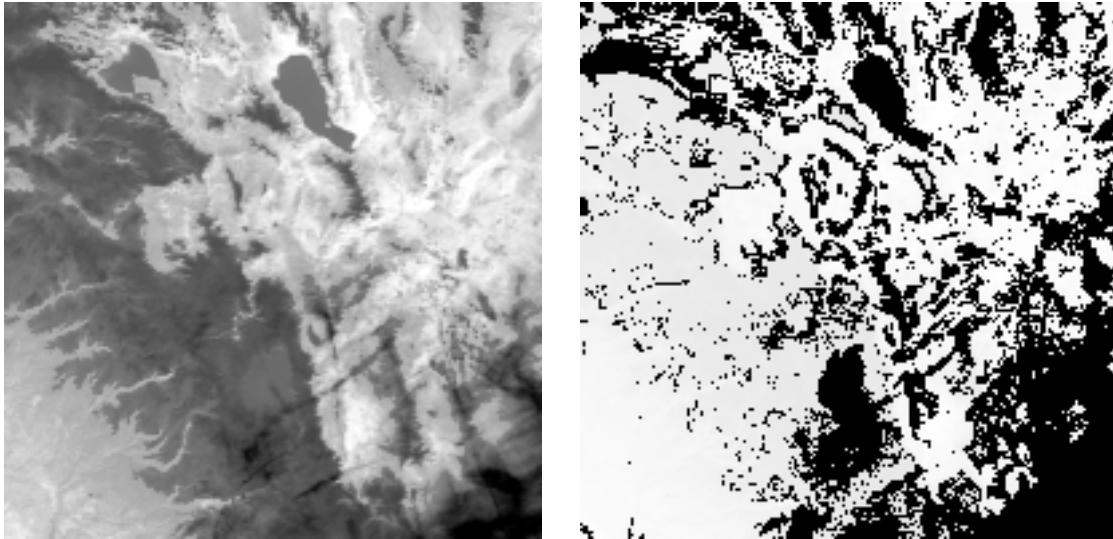


Figure 6. Daytime MODIS scene acquired over Lake Tahoe on 3/12/2000. Image on left is a grayscale brightness temperature image from the band 31 and image on right is the MODIS surface temperature product.

These results have been discussed with the algorithm developers for both the cloud mask and surface temperature products and both developers are looking for a solution. In the case of the cloud mask, any change will have ramifications for many other products, since most of the MODIS products utilize the mask and so any changes will be made with caution. Further, in principal the mask is working correctly since it is identifying cloud-free pixels. Similarly a change to the surface temperature product could result in pixels being processed that are in-fact cloudy and erroneous values being provided, potentially reducing the overall quality of the product. However, it is important that a solution be found since these problems limit the value of the land surface temperature/emissivity product to the land community.

Surface Emissivity Product (MOD11_L2, AST08)

The procedure for validating the surface emissivity product was outlined in the previous section. Like the surface temperature product, the accuracy of the surface emissivity product will vary with cover type and atmospheric conditions. Therefore it is important to validate this product over a range of cover types and conditions. Thus far this product has been validated over one-cover types: water. Other cover types include grassland (Uardry site) and bare soil (Amburla site). Other atmospheric conditions include the Thangoo site (high water vapor). Figure 7 illustrates the results of validating the ASTER surface emissivity over Lake Tahoe.

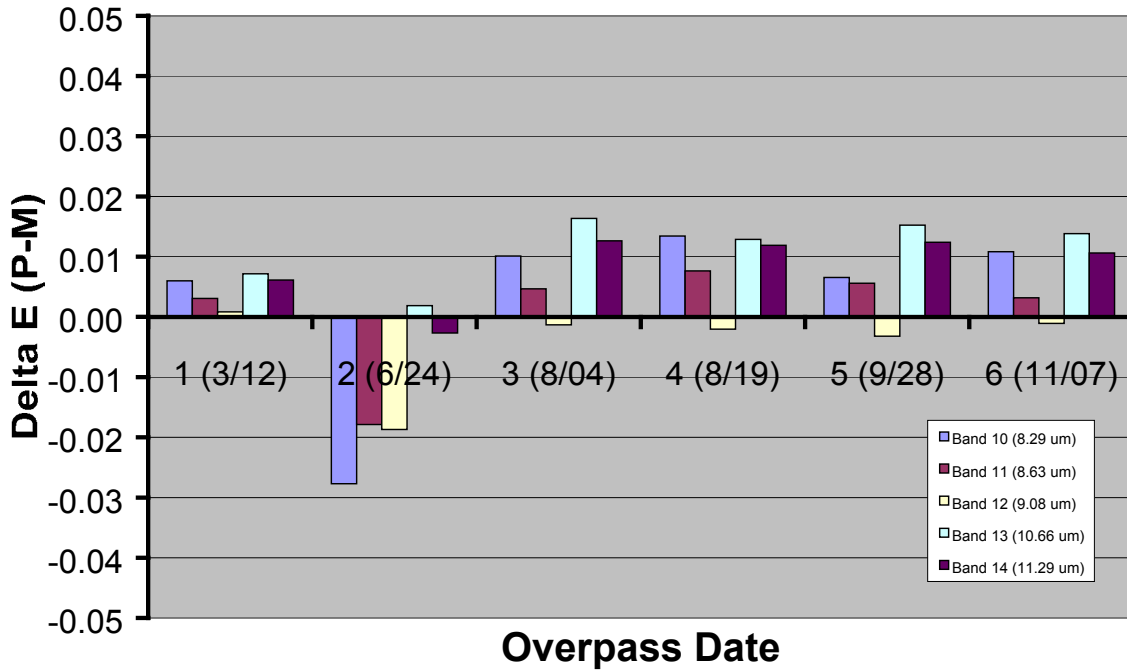


Figure 7. Emissivity Difference between ASTER Predicted and Measured Values over Time CY2000 v1.0.2

Examination of this figure indicates that for this cover type generally there appears to be a positive bias, except for 6/24/00. In order to understand the result for 6/24/00 it is important to understand how the ASTER surface temperature/emissivity algorithm works. Basically the algorithm performs an initial test to determine if the material is water or land. If the pixel is identified as water then a different processing path is taken than if it is identified as land. On 6/24/00 the water was incorrectly identified as land and took a different path through the algorithm with different assumptions and different emissivities. The ASTER temperature/emissivity retrieval algorithm developers anticipated that these effects would occur and are using these data to “tune” the ASTER algorithm.

No results are presented for the MODIS surface emissivity product for the same reasons discussed with the surface temperature product.

Validation Summary Tables

This section summarizes the results from the ongoing validation of the ASTER and MODIS thermal infrared data and products. It is important to recognize that this is a work in progress and future reports will include additional detail. Table 3 below summarizes the accuracy of the radiance at sensor product for MODIS and ASTER in the “window” channels. These results suggest that there is not a strong bias in either the MODIS or ASTER radiance at sensor products for the “window” channels and in terms of preflight

calibration accuracy, given the caveats listed under Notes for Table 3 both instruments have exceeded specification.

Instrument	Band And Center (um)	Preflight Calibration Accuracy Req. ¹	Validated Accuracy Mean of % Difference (%) ^{2, 3,4,5}	Validated Accuracy Mean of BT Difference (K) ^{3,4,5}	Validated Accuracy Std. Dev. of % Difference (%) ^{2, 3,4,5}	Validated Accuracy Std. Dev of BT Difference (K) ^{2, 3,4,5}
MODIS	29 (8.53)	<1%	0.57	0.27	0.58	0.28
MODIS	31 (11.02)	<1%	0.27	0.17	0.51	0.31
MODIS	32 (12.03)	<1%	0.38	0.25	0.48	0.32
ASTER	10 (8.29)	≤1 K	0.69	0.32	0.52	0.24
ASTER	11 (8.63)	≤1 K	0.49	0.24	0.36	0.18
ASTER	12 (9.08)	≤1 K	0.44	0.22	0.36	0.19
ASTER	13 (10.66)	≤1 K	0.09	0.06	0.34	0.20
ASTER	14 (11.29)	≤1 K	0.32	0.20	0.33	0.21

Table 3. Preflight and Validated Accuracy of the ASTER and MODIS radiance at sensor products for nadir viewed scenes. Preflight calibration accuracy requirements for MODIS and ASTER are obtained from Barnes et al., 1998 and Fujisada et al., 1998.

Notes for Table 3

- ¹. The ASTER preflight calibration accuracy requirement is for the 270-340 K range.
- ². The % difference is calculated as the (Predicted-Measured)/Predicted)*100 where the predicted is derived from the field measurements and the measured is the satellite values.
- ³. The results are for scenes in the radiance range 6.8-8.3 W/m²/sr/μm, brightness temperature range 278-290K using MODIS channel 31 as a reference.
- ⁴. All scenes used were nadir views and the Table 3 does not include differences due to view angle (e.g. response versus scan angle for MODIS).
- ⁵. Different sized areas were used for the retrievals due to the different spatial resolutions of the 2 instruments (see text for details).

Table 4 summarizes the results for the ASTER surface temperature product using Lake Tahoe. Results are not reported for the MODIS land surface temperature/emissivity product for the reasons discussed in the previous section. The results for the ASTER temperature product exceed the preflight specification. However, it is important to realize that product accuracy varies with cover type and water is likely to provide the best accuracy. Further work will focus on validating the accuracy of the product for the other cover types characterized by the Australian sites.

ASTER Surface Temperature Product (AST08)			
Cover Type	Preflight Product Accuracy Requirement (K)	Validated accuracy Mean of Temperature Difference (K) ^{1,2}	Validated accuracy Std. Dev of Temperature Difference (K) ^{1,2}
Water	± 1.5	-0.95	0.44

Table 4 Preflight and Validated Accuracy of the ASTER surface temperature product (AST08) over water. Preflight accuracy requirement obtained from Gillespie et al. 1998.

Notes for Table 4

1. The temperature difference is calculated as the (Predicted-Measured) where the predicted is the satellite derived and the measured is the field measured.
2. The accuracies are for scenes in the kinetic temperature range 279-292K.

Table 5 summarizes the results for the ASTER surface emissivity product using Lake Tahoe. Results are not reported for the MODIS land surface emissivity product for the reasons discussed in the previous section. Again the results for the ASTER emissivity product exceed the preflight specification. However, it is important to realize that product accuracy varies with cover type and water is likely to provide the best accuracy. Further work will focus on validating the accuracy of the product for the other cover types characterized by the Australian sites.

ASTER Surface Emissivity Product (AST08)			
Cover Type Water	Preflight Product Accuracy Requirement (K)	Validated accuracy Mean of Emissivity Difference (K) ^{1,2}	Validated accuracy Std. Dev of Emissivity Difference (K) ^{1,2}
Band 10	± 0.015	0.003	0.015
Band 11	± 0.015	0.001	0.009
Band 12	± 0.015	-0.004	0.007
Band 13	± 0.015	0.011	0.006
Band 14	± 0.015	0.008	0.006

Table 5 Preflight and Validated Accuracy of the ASTER surface emissivity product (AST08) over water. Preflight accuracy requirement obtained from Gillespie et al. 1998.

Notes for Table 5

1. The emissivity difference is calculated as the (Predicted-Measured) where the predicted is the satellite derived and the measured is the field measured.
2. The accuracies are for scenes in the emissivity range 0.983-0.991.

Future Plans

- 1) Validate ASTER and MODIS thermal infrared data and products at all sites (ongoing).
- 2) Replace TR3 and TR2 with ocean-going buoys supplied by NOAA. These buoys have a far greater lifetime than the existing rafts (Fall 2001).
- 3) Replace TR1 and TR4 with new ocean-going buoys. This effort is dependant on additional external funding. If funding cannot be obtained these rafts will be retrieved for the winter to avoid damage associated with winter storms (Fall 2001).
- 4) Add meteorological station to TR2. Meteorological station will include wind speed, wind direction, relative humidity, pressure and a net radiometer. This will provide a meteorological station on the western and eastern side of the lake.
- 5) Re-deploy land instrumentation as US Coast Guard Pier.
- 6) Establish a calibration protocol for all instruments, especially the radiometers and temperature loggers. This will involve cross comparison of the instrumentation developed for the Australian and US sites. This task is ongoing and will involve further comparisons similar to those made in Miami against the NIST blackbody as discussed in the report.

The following items were completed in FY 2001 as scheduled.

- 1) Validate ASTER and MODIS thermal infrared data and products at all sites (ongoing).
- 2) Replace Mk II radiometers with Mk III radiometers. The Mk III radiometers include a nulling blackbody and should be more accurate than the Mk II radiometers.
- 3) Add meteorological station to TR3. Meteorological station will include wind speed, wind direction, relative humidity, pressure and a net radiometer.
- 4) Establish a calibration protocol for all instruments, especially the radiometers and temperature loggers. This will involve cross comparison of the instrumentation developed for the Australian and US sites (ongoing).
- 5) Deploy scanning radiometer at Amburla site.
- 6) Re-installation of equipment at Thangoo site damaged by fire and cyclones.

Schedule

The Tahoe, Amburla, Thangoo and Uardry sites are now fully operational and the highest priority task is to validate the thermal infrared data and products from MODIS and ASTER. This will be ongoing since we want to obtain cloud-free data over a range of temperatures. There are several other tasks, all of which involve improvements to the infrastructure or instrumentation at the sites, and the approximate time for these is listed with the future plans.

Publications and Media

- Hook, S. J. 1998. In Flight Validation of Thermal Infrared Data over Land. European Symposium on Remote Sensing: SENSORS, SYSTEMS AND NEXT GENERATION SATELLITES IV, Barcelona, Spain, September 21-25. (Abstract).
- Hook, S. J., Schladow, G., Abtahi, A. F. Prata and B. Richards. In-Flight Validation of Remotely Sensed Thermal Infrared Data for Hydrological Applications. American Geophysical Union, San Francisco. (Abstract)
- Hook, S. J., G. Schladow, A. Abtahi, F. Prata, B. Richards and S. Palmansson. Validation of ASTER and MODIS Thermal Infrared Products. Sixth International Conference Remote Sensing for Marine and Coastal Environments. Charleston, South Carolina, May 1-3 2000. (Abstract)
- Hook, S. J. 2000. MASTER – A New Instrument for Hyperspectral Analysis from the Visible to Thermal Infrared. 2nd EARSel Workshop on Hyperspectral Imaging, Enschede, The Netherlands, July 11-13. (Abstract).

- Hook, S. J., Myers, J. J., Thome, K. J., Fitzgerald, M. and A. B. Kahle, 2001. The MODIS/ASTER Airborne Simulator (MASTER) – A New Instrument for Earth Science Studies. *Remote Sensing of Environment*, vol. 76, Issue 1, pp. 93-102.
- Hook, S. J. Thome, K. J., Myers J. J. and M. Fitzgerald, 2000. In Flight Validation of MASTER Data – A Necessity for Quantitative Geologic Mapping. Fourteenth International Conference and Workshops on Applied Geologic Remote Sensing, Las Vegas, Nevada, November 6-8, 2000. (Abstract)
- Hook, S. and F. Prata, 2001. Land Surface Temperature Measured by ASTER and MODIS - First Results. European Geophysical Society, 26th General Assembly, Nice, France, March 25-30 2001. (Abstract)
- Hook, S. Schladow, G. Abtahi, A., Alley, R. and R. Richards, 2001. In-Flight Validation of Remotely Sensed Thermal Infrared Data using an Automated Validation Site – Lake Tahoe, CA. Workshop on Multi/Hyperspectral Image Compression and Analysis, Redstone Arsenal, Huntsville, Alabama, September 18-20, 2001.
- Hook, S. J., Prata, F. J., Alley, R. E., Abtahi, A., Richards, R. C., Schladow, G. S. and S. O. Palmarsson, 2001. Retrieval of Lake Bulk-and Skin-Temperatures using Along Track Scanning Radiometer (ATSR) Data: A Case Study using Lake Tahoe, CA.
- Tahoe World January 13 2000. 1.3 billion satellite links Tahoe to NASA *By Shannon Darling, Tahoe World Staff.*
- Tahoe World March 10, 2000. NASA rafts await satellite data *By Shannon Darling, Tahoe World Staff.*

Collaborations

Strong collaborations have been established with the EOS instrument teams (ASTER, MODIS and Landsat) as well as other instruments such as Multispectral Thermal Imager developed by the Department of Energy and Along Track Scanning Radiometer developed by the Rutherford Appleton Laboratory and flown on a European platform. One example of a particularly valuable collaboration is with Liam Gumley at the University of Wisconsin. Gumley is responsible for the MODIS direct broadcast data received by the UW and has set up a script that automatically sends a subset of the MODIS 1B direct broadcast data covering Lake Tahoe by FTP push for every overpass. These data are invaluable since they provide the few kilobytes of data needed for the validation rather than the ~ 600 mb of data that must be downloaded to validate one overpass when data are obtained from the DAAC. Strong collaborations have also been developed with other colleagues at the University of Wisconsin: Chris Moeller for Level 1B validation and Richard Fry for the Cloud Mask. Nazmi El Zaleous at the Goddard DAAC has also been helpful in getting the early MODIS scenes reprocessed.

Archiving

A web site has been established which is the primary mechanism for disseminating information. All data on the site are backed up as part of the main ASTER archive over the network and also locally on a nightly basis. In addition the MODIS instrument team designated Lake Tahoe an EOS Core Site in CY2000, primarily thanks to Jeff Morisette on the MODIS land validation team. As a result of this designation a large amount of data associated with the site is being made available online. Efforts are also being made to include the validation information at this site:

<http://modis-land.gsfc.nasa.gov/val/>

Note: Both Lake Tahoe and Uardy are now designated as EOS Core Sites.

WebPages

<http://shookweb.jpl.nasa.gov/validation>

<http://modis-land.gsfc.nasa.gov/val/>

<http://blt.wr.usgs.gov/>

References

Barnes, W. L., Pagano, T. S. and V. V. Salomonson, 1998. Pre-launch characteristics of the Moderate Resolution Imaging Spectroradiometer (MODIS) on EOS AM1. *Trans. Geosci and Remote Sens.* 36:1088-1100.

Gillespie, A., Rokugawa, S. Matsunaga, T., Cothorn, S, Hook, S. and A. Kahle, 1998. A Temperature and Emissivity Separation Algorithm for Advanced Spaceborne Thermal Emission and Reflectance Radiometer (ASTER) Images. *IEEE Transactions on Geoscience and Remote Sensing*, vol. 36 pp. 1113-1126.

Fujisada, H., Sakuma, F., Ono, A. and M.Kudoh, 1998. Design and Preflight Performance of the ASTER Instrument Protoflight Model. *Trans. Geosci and Remote Sens.* 36:1152-1160.

Kannenber, B. (1998), IR Instrument Comparison Workshop at the Rosenstiel School of Marine & Atmospheric Science (RSMAS). *The Earth Observer.* 10.